ELSEVIER

Thermochimica Acta 374 (2001) 171–184

thermochimica acta

www.elsevier.com/locate/tca

Thermodynamics of a complex melting process: the case of spironolactone

A. Marini*, V. Berbenni, G. Bruni, A. Maggioni, A. Orlandi[1], M. Villa[2]

C.S.G.I. e CSTE-CNR, Dipartimento di Chimica Fisica, Università degli Studi di Pavia, Viale Taramelli 16, 27100 Pavia, Italy

Received 30 October 2000; received in revised form 12 March 2001; accepted 13 March 2001

Abstract

An investigation of ''melting'' in spironolactone under different experimental conditions demonstrates that the melting is always accompanied by loss of mass, and by an endothermic and temperature-activated ''decomposition'' process. However, experiments performed under different atmospheres reveal a more complex phenomenology than expected for a simple melting/decomposition process. It is shown that the byproducts of decomposition may undergo an exothermic process, which we will call ''oxidation''. The ''oxidant'' may be the oxygen of the atmosphere or may be provided by decomposition. By combining a number of experiments, we estimate the melting enthalpy, the specific enthalpy of decomposition and that of oxidation. We show that an ''adiabatic'' balance between decomposition and oxidation is eventually attained. The concept of ''adiabatic balance'' provides simple explanations for several experimental observations.

Keywords: Thermodynamics; Melting; Decomposition; Oxidation; Thermal methods; Spironolactone

1. Introduction

In this paper we will deal with the complex melting behavior of a well-known substance, spironolactone, a diuretic drug with steroid structure. Agafonov et al. [1] claimed that pure spironolactone exists in two polymorphic forms, with slightly different enthalpies and temperatures of melting; these authors also characterized four solvated crystalline forms of the drug. The existence of several forms of spironolactone was believed to be responsible for the widely different data regarding its bioavailability [2,3], which is controlled by a low solubility in water. In a previous work, we have completed a characterization of the so-called ''forms'' of spironolactone [4]. We have found details in the X-rays diffraction patterns and IR spectra that allow to identify two ''forms'' with significant, but minor, structural differences. On the other hand, the claim of Agafonov et al. [1] could not be confirmed: while details of the thermal response appear to be influenced by preparation and treatments, we found no evidence of a relationship between melting behavior and X-rays/IR signatures. Under the same experimental conditions, all of our samples display almost the same thermal behavior in the melting region. Since differences between the forms of spironolactone are not relevant in the context of this work, we will present only data obtained with the original and untreated commercial compound.

* Corresponding author. Tel.: +39-382-507-219; fax: +39-382-507-670.
E-mail address: marini@matsci.unipv.it (A. Marini).
[1] Present address: GlaxoWellcome, Medicines Research Center, Via A. Fleming 2, 37135 Verona, Italy.
[2] Present address: Unità INFM, 27100 Pavia, Italy.

0040-6031/01/$ – see front matter
PII: S0040-6031(01)00500-7

The focus of the paper is on simultaneous DSC/TGA measurements, by which both enthalpy and mass changes can be obtained. We feel this is useful in the case of organic substances, whose thermal phenomena often involve processes which bring about changes of composition (e.g. chemical reactions, solvent evaporation, decomposition).

For the non-solvated forms of spironolactone studied in the literature, melting temperatures between 478 and 483 K, with melting enthalpies in the (48–53) J g^{-1} interval have been reported [1]. In a first run with over 11 samples,[3] we actually obtained 50.8 ± 1.5 J g^{-1} for the melting enthalpy, in apparent overall agreement with the literature. Subsequently, we found that, by decreasing the heating rate, very different results for both the enthalpy and the onset of the ''melting'' were obtained. Furthermore, the loss of mass during the melting process was below 0.5% at rates $\geq$10 K min^{-1}, but it was several percents of the sample mass at rates below 1 K min^{-1}. At scanning rates below 10 K min^{-1}, both loss of mass and ''melting'' enthalpies strongly depend upon the atmosphere (air or nitrogen). Finally, for equal scanning rates, the ''melting'' enthalpy is decreased by hours-long annealing around 443 K. All these phenomena will be discussed in detail below. We will also quote, when pertinent, results from other measurements (SEM, DSC, MTDSC, TG/FT-IR). An interpretative model will then be introduced and discussed.

2. Experimental

Spironolactone of high purity (99.97%) from a single industrial batch (Sigma Chimica) was used as received. At the scanning electron microscope (SEM), the powder presents grains with size up to about 2 μm, and sub-micron particles with characteristic rounded shapes (Fig. 1).

Thermal analyses have been performed with a range of instruments under different conditions. Samples mass was around 4 mg and was kept constant as much as possible.

- In the Du Pont 910 differential scanning calorimeter (DSC), the samples were sealed in an aluminum capsule; unless otherwise noted, the top of the capsule was manually pierced with a pin before sealing and the atmosphere was a flow of dry nitrogen (30 ml min^{-1}). Heating rates in the 0.3–50 K min^{-1} range were used for these DSC measurements. The module was interfaced with a TA 2000 data station (TA Instruments, USA).
- Simultaneous DSC and thermogravimetric (TGA) analyses (STA in the following) where performed with the STA 625 system of Polymer Laboratories (UK). The container of the sample was an aluminum cylinder, low and without top, which allowed a much better contact with the atmosphere of the measuring chamber (still air or nitrogen flow of 40 ml min^{-1}) than the sample in the pierced capsules for the Du Pont 910. Heating rates from 0.3 to 50 K min^{-1} were used.
- DSC measurements with temperature modulation (MTDSC) were made with model 2920 by TA Instruments, interfaced with a TA3100 data station (TA Instruments, USA). The sample was sealed in an aluminum container with the top manually pierced by a pin (pierced pan). As for the Du Pont DSC, the atmosphere was a flow of dry nitrogen (30 ml min^{-1}). The period of modulation was 40 s, while the underlying heating rates were 2 and 3 K min^{-1} and the temperature amplitudes were 0.212 and 0.318°C, respectively. With these parameters the instantaneous temperature rate oscillates between 0 and two times the underlying heating rate.
- An infrared Fourier transform spectrometer (FT-IR 730 by Nicolet, USA) was connected with the Du Pont 951 TGA cell for simultaneous TG/FT-IR measurements. We used nitrogen as the carrier gas (at 50 ml min^{-1}) and heating rates from 2 to 10 K min^{-1}. The infrared cell was kept at 571 K; the spectra in the interval (4000–500 cm^{-1}) were acquired with a 16 cm^{-1} resolution by a DTGS detector.

[3] The samples were scanned at heating rates of 5, 10, 20 and 50 K min^{-1}.

3. Results

3.1. The melting region

3.1.1. Enthalpy and mass changes

Fig. 2 compares simultaneous thermal analyses (STA) at a high scanning rate (50 K min^{-1}, upper part, a) and a low scanning rate (0.3 K min^{-1}, lower

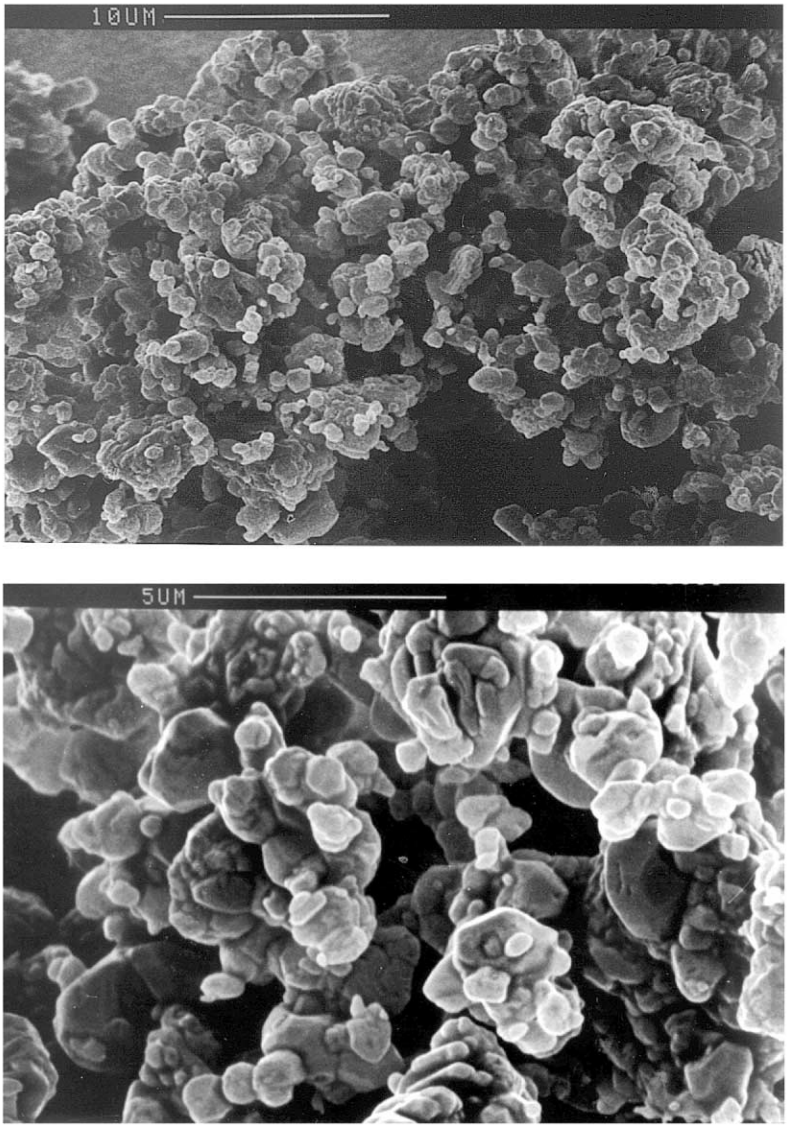

Fig. 1. SEM micrographs of spironolactone powders.

part, b) obtained with samples in open pan and in a nitrogen flow. At 50 K min^{-1}, the onset temperature of the single endothermic peak is $T_e = 478.5$ K and the peak reaches a maximum at $T_{1p} = 484.5$ K. From this peak an enthalpy of 51 J g^{-1} is obtained, in agreement with the literature. As customary, the onset temperature (T_e) is obtained as the crossing point between the baseline and the tangent at the low-temperature side of the curve in the flex point, the enthalpy is determined by integration between points 1 and 2 identified in the curve. Here and in the following, the change of mass Δm between points 1 and 2 is divided by the initial mass m_{in} to obtain the fractional change of mass during the thermal phenomenon

$$m_1 \equiv \frac{\Delta m}{m_{in}}$$

where m_1 is 0.3% in Fig. 2a.

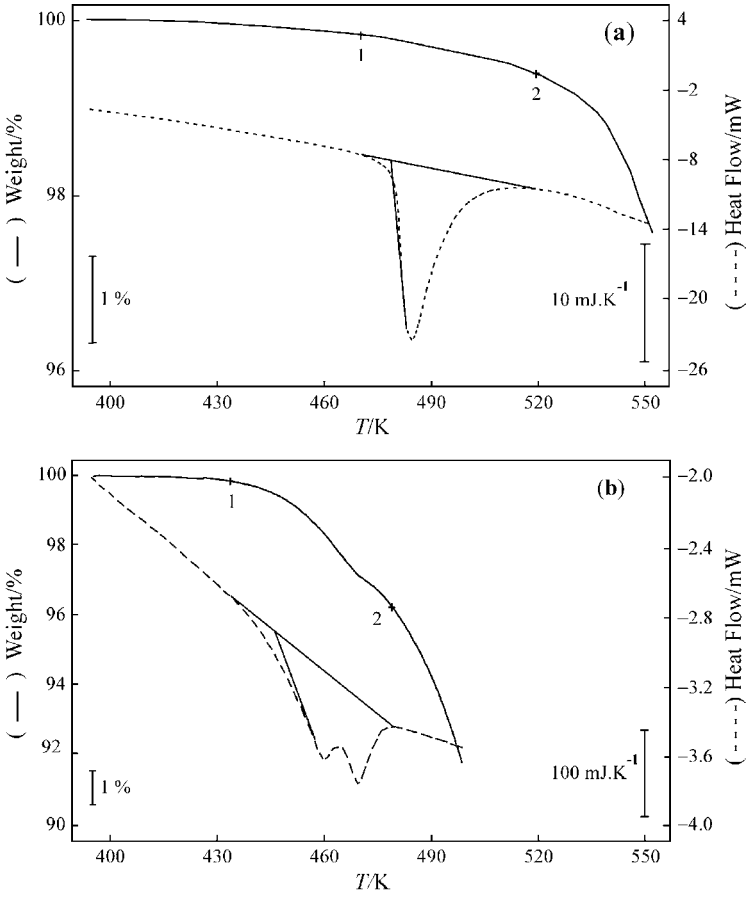

Fig. 2. Simultaneous TGA (left axes) and DSC (right axes) recordings at 50 K min^{-1} (upper part, a) and 0.3 K min^{-1} (lower part, b) with samples weighting 4.2 ± 0.1 mg. The sticks with the vertical units call the attention to the different vertical scales used in (a) and (b); the heat fluxes are represented in (mW) but the corresponding sticks have been translated into (mJ K^{-1}) by division with β.

The situation has dramatically changed at a heating rate of 0.3 K min^{-1}: T_e has now dropped to 446 K, the endothermic phenomenon produces two maxima, the first at $T' = 459$ K and the other at $T_{1p} = 469$ K (Fig. 1b). The area between baseline and DSC peak between points 1 and 2 corresponds to an enthalpy $\Delta H_1 \cong 420$ J g^{-1}, nearly ten times the enthalpy obtained from Fig. 2a. The mass is apparently lost in two distinct steps, and the overall loss of mass is now $m_1 \approx 3.5\%$.

Fig. 3a presents, as a function of the heating rate, the behavior of T_{1p} and T_e while those of the enthalpy ΔH_1 and the change of mass m_1 are shown in Fig. 3b. Both m_1 and ΔH_1 increase rapidly with decreasing heating rate (β) below 5 K min^{-1}. T_{1p} and T_e shift towards low temperatures with decreasing β and, below 1 K min^{-1}, two distinct peaks appear. For the one at high temperature we have maintained the symbol of T_{1p} for the temperature of its peak (see Fig. 3) and indicated the temperature of the first maximum with T'. The growth of ΔH_1 and the shift of T_e with lowering heating rates are both unexpected for a melting process.

The error bars for ΔH_1 and m_1 at $\beta = 0.5$ K min^{-1} in Fig. 3b are the deviations of data collected over a dozen of runs. These deviations are mostly due to intrinsic run-to-run variability. The correlation between these quantities is stronger than implied by Fig. 3b in the sense that fluctuations of ΔH_1 (J g^{-1}) at $\beta = 0.5$ K are coupled with the fluctuations of m_1 at the same heating rate. This becomes evident if the

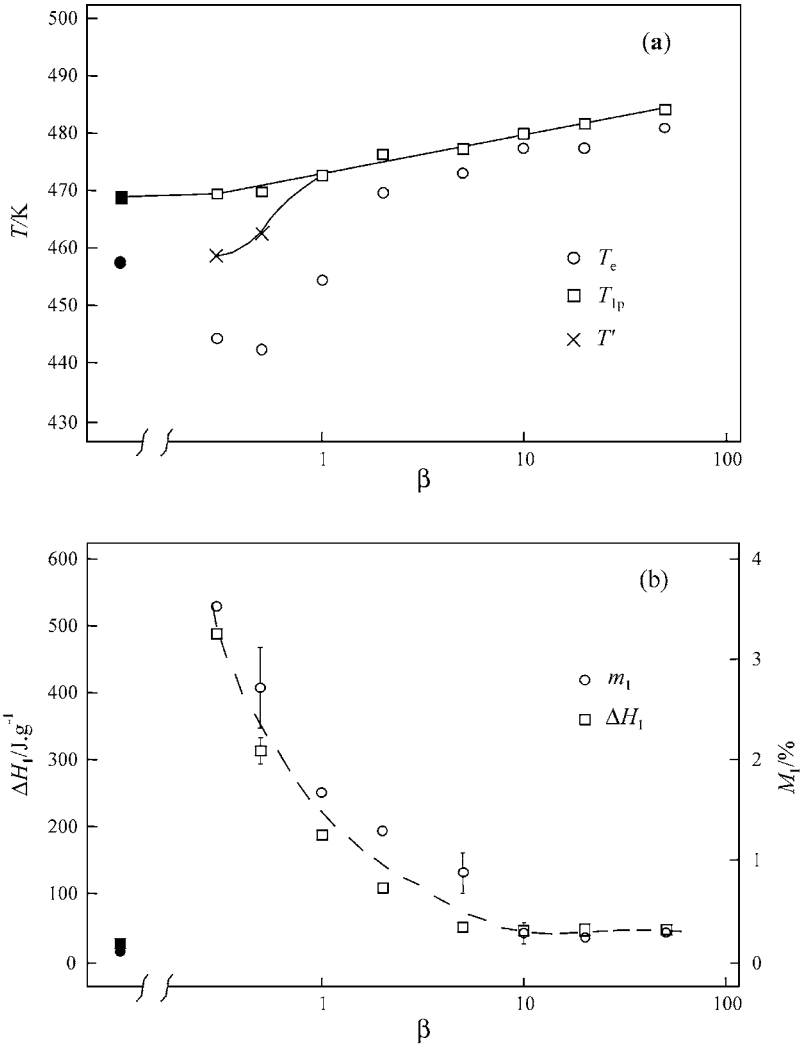

Fig. 3. (a) Behavior of T_{1p} and T_e as a function of β; T' (×) is the temperature of the peak observed at low-temperature below 1 K min^{-1}; (b) behavior of m_1 and ΔH_1 as a function of β; the filled symbols represent the results of the annealing experiments described in the text.

enthalpy changes are represented as a function of the corresponding changes of mass. Regression analysis of these data yields

$$\Delta H_1 = A + Bm_1 \quad (1)$$

where $A = 28.6 \pm 4.8$ J g^{-1} and $B = 10.06 \pm 0.26$ kJ g^{-1}. The correlation coefficient is 0.994, meaning there is a very good correlation between enthalpy and mass changes. Eq. (1) shows that the measured enthalpy changes result from the sum of a constant contribution and a mass-dependent contribution.[4] We believe this last one is responsible of the unexpected behavior of both ΔH_1 and T_e with lowering heating rates and of the appearance of the low temperature endothermic peak.

[4] Eq. (1) does not correctly describe the behavior at high scanning rates: from 10 to 50 K min^{-1}, the enthalpies are nearly constant (∼50 J g^{-1}) while m_1 goes from ∼0.4 to ∼0.1%. The reason will be explained in the following.

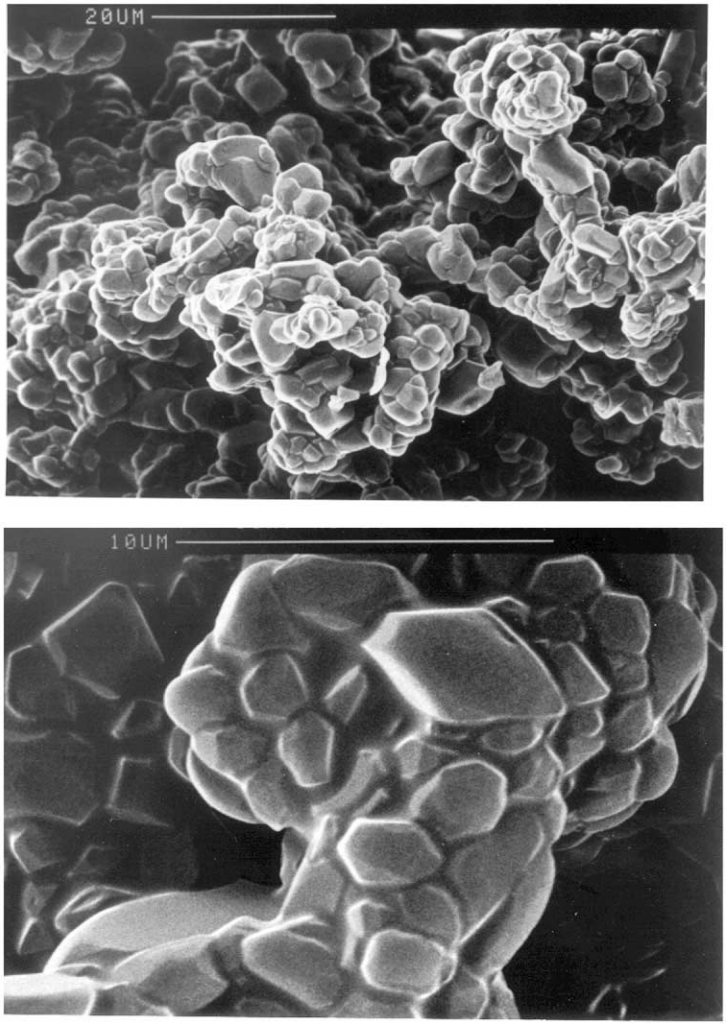

Fig. 4. SEM micrographs of a spironolactone sample annealed (pierced pan) in nitrogen 5 h at 443 K.

Further information about the nature of these thermal phenomena are obtained by studying a sample that has been annealed (pierced pan) in nitrogen 5 h at 443 K (i.e. near T_e of Fig. 2b) before being brought at 373 K and scanned at 5 K min^{-1}. Micrographs of an annealed sample are reported in Fig. 4. A comparison with Fig. 1 shows that significant morphological changes take place as a consequence of the annealing. The sample annealed and scanned as described had a single endothermic peak with $T_e = 458$ K, $T_{1p} = 469$ K and $\Delta H_1 = 30$ J g^{-1}. Furthermore, less than 0.1% of mass was lost during the measuring run. Very similar results were obtained with longer annealing times (measurements were made with annealing times up to 16 h). Thus, when the mass-dependent contribution to the enthalpy change is eliminated by annealing, we obtain the ΔH_1 value predicted by Eq. (1) for zero mass loss. The mass loss that usually occurs in the melting region takes place during annealing so that, when scanned, the annealed samples do not show any significant mass loss during melting. It is reasonable to think that the same result could be obtained avoiding the annealing, but scanning samples at very low heating rates. On this basis, it seems appropriate to represent the data of the run with the annealed sample as points corresponding to very small

heating rates (full symbols in the left sides of Fig. 2a and b). We believe that these data roughly represent the behavior expected for the high temperature peak for $\beta \rightarrow 0$.

Our results suggest that what appears as a single "melting peak" at high scanning rates results from superposition of two distinct phenomena: a kinetically controlled endothermic process (decomposition), which is always associated with loss of mass, and another phenomenon which is weakly dependent upon β, and, in the limit of very small scan rates, appears to have $T_e = 458$ K and to require about 30 J g^{-1}.

Furthermore, melting is apparently irreversible for samples heated in open or pierced pans. Instead, the thermal response of samples previously melted in closed containers is similar to that of samples annealed at 443 K.

3.1.2. The role of the atmosphere

Several measurements with the STA system have been repeated in still air with samples in open containers. For $\beta \geq 5$ K min^{-1}, enthalpies and mass losses are not significantly different from the corresponding quantities measured under a nitrogen flow. For lower heating rates, the enthalpy in air decreases and the loss of mass increases, relative to corresponding experiment in N_2. For example, at $\beta = 0.5$ K min^{-1} ΔH_1 is 330 ± 30 J g^{-1} in N_2 and 190 J g^{-1} in air while m_1 is $3.0 \pm 0.2\%$ in nitrogen and 3.5% in air. Since our decomposition is an endothermic process, both enthalpy and mass loss were expected to change in the same direction (see Eq. (1)). Their opposite trends suggest that, besides decomposition, an exothermic process takes place which is enhanced by the presence of O_2 in the atmosphere: we will call this process "oxidation".

To show that oxidation may act upon the byproducts of decomposition even under a nominally inert atmosphere, we compare experiments performed under dry N_2, one time in an open pan (STA system) and another time in a pierced pan. When decomposition occurs, the atmosphere inside the pierced pan may differ substantially from the external atmosphere. At high heating rates, a constant enthalpy of about 50 J g^{-1} is obtained in both open and pierced pans. For heating rates below 2 K min^{-1}, T_{1p} decreases slightly (exactly as it did in the open pans, see Fig. 3a) but ΔH_1 now decreases, in striking contrast with the behavior reported in Fig. 3. In particular, ΔH_1 has a value of 36 J g^{-1} at 0.5 K min^{-1}, i.e. about one-tenth the ΔH_1 value in the open pan at the same scanning rate. The above suggests that in a pierced pan at low heating rates, the contribution of oxidation is much more important than in the open pan.

Fig. 5a and b present MTDSC runs performed with samples in pierced pans at average temperature rates of 2 and 3 K min^{-1}, respectively. MTDSC can be considered an evolution of conventional DSC, where a sinusoidal modulation of temperature is added to the conventional heating/cooling ramp. In principle, MTDSC gives a better insight of the thermal phenomena since discriminates between reversing and non-reversing contributions [5–7]. The deconvolution of the modulated heat flow into reversing and non-reversing components is based on the assumption that all thermally reversing phenomena contribute to heat capacity. Thus, a careful heat capacity calibration is always needed to separate reversing and non-reversing effects in MTDSC. However, the heat capacity calibration constant strongly depends on the modulation period [8]. Moreover, the response to modulation of a physico-chemical transformation will depend on the nature of the transformation and on the modulation conditions themselves. As a consequence, while the total heat flow obtained by MTDSC has the same meaning and quantitative reliability as in conventional DSC, its deconvolution into reversing and non-reversing components has poor quantitative reliability [9,10]. Even with the above limitations, the comparison of MTDSC data collected at the same modulation period can give useful information. Assuming, as it seems reasonable, that the non-reversing contribution to the total heat flow is mainly due to decomposition/oxidation, we can assign to decomposition the first thermal event of Fig. 5a (which is almost entirely non-reversing). Here, the reversing portion contributes mainly to the second thermal event (melting + decomposition/oxidation), during which the non-reversing contribution accounts, in the average, for more than half the total heat flow.[5]

[5] The total area of the two peaks of Fig. 5a corresponds to an enthalpy change of 52 J g^{-1}. The area of the second peak is estimated to correspond to 40 J g^{-1} and the non-reversing part of this peak is estimated 22 J g^{-1}. We stress, however, that melting itself may give a non-reversing contribution to the total heat flow.

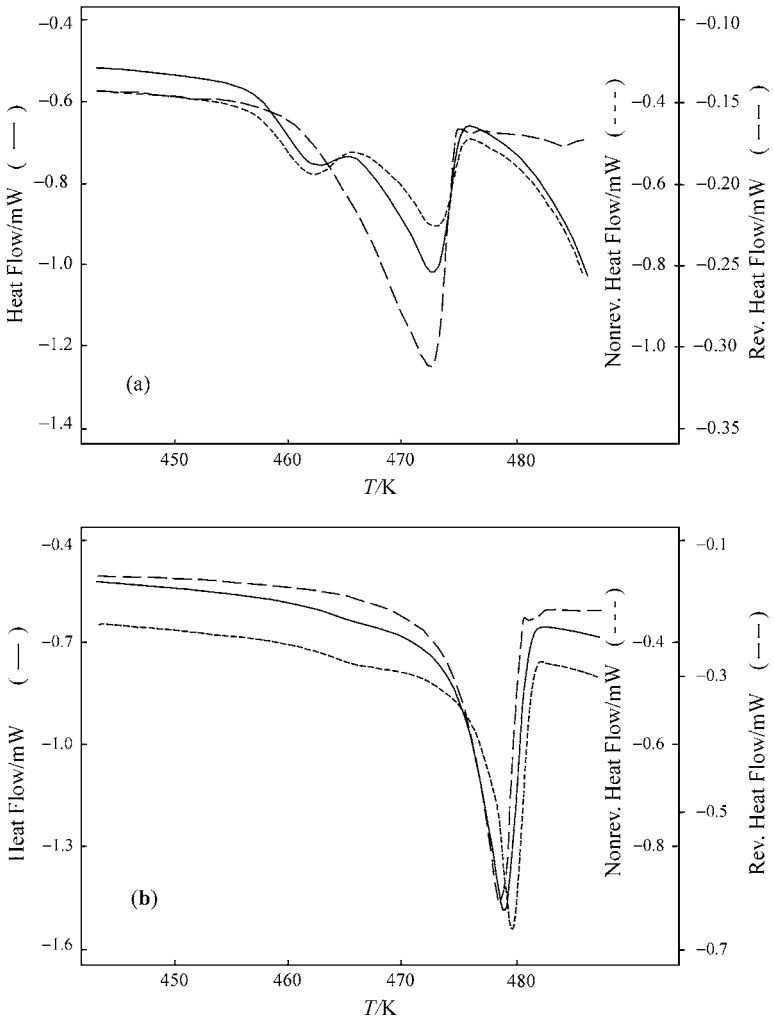

Fig. 5. Total heat fluxes and their reversing and non-reversing components as determined by MTDSC experiments performed at an average heating rate of 2 K min^{-1} (upper) and 3 K min^{-1} (lower).

When the average heating rate is raised to 3 K min^{-1} (Fig. 5b) the initial non-reversing thermal effect nearly disappears, confirming that it strongly depends upon the heating rate. Moreover, peak temperatures are shifted to substantially higher values and the non-reversing part accounts now for half of the total enthalpy of 48 J g^{-1}. These changes confirm that: (a) the initial thermal event of Fig. 5a is due to decomposition/oxidation; (b) decomposition/oxidation shifts towards higher temperatures with increasing heating rate. Last, we note that after the peak, the "baseline" of the reversing contribution is essentially flat both in Fig. 5a and b. This confirms that the reversing contribution to the total heat flow during the peak was due to melting. On the other hand, the baselines of the total heat flow and of its non-reversing part are bent in the endothermic direction, but they are much flatter in Fig. 5b than in Fig. 5a. This suggests that non-reversing thermal events, namely decomposition/oxidation, are occurring after the peak and that the resulting thermal effect depends on the experimental conditions. What happens above the melting

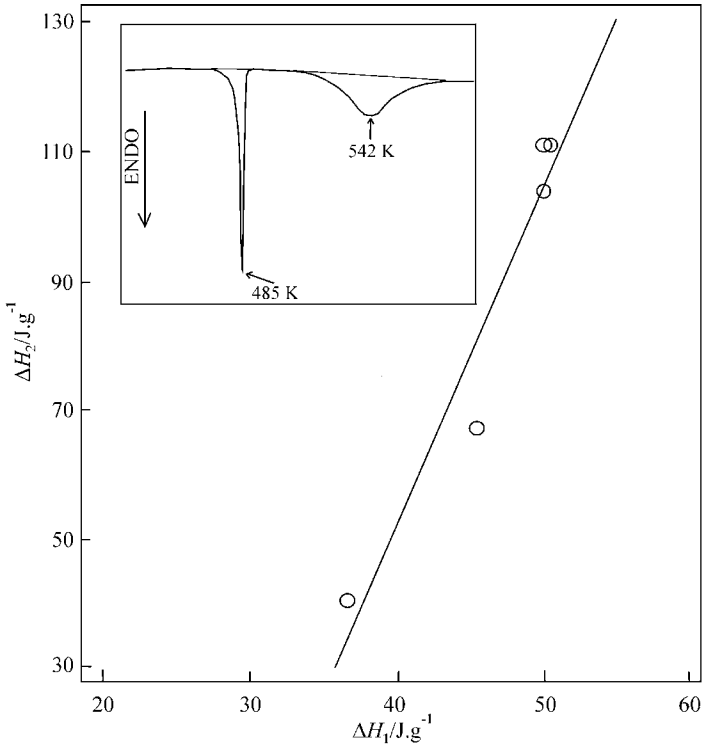

Fig. 6. Relationship between ΔH_1 and ΔH_2 measured in the same DSC run in a pierced pan. A typical DSC recording is shown in the inset ($\beta = 5$ K min^{-1}). The data have been collected over the 0.5–5 K min^{-1} range of β values.

will be better discussed in the following. We note here that MTDSC results provide support for the picture deduced from conventional thermal measurements.

3.2. Above the melting

After melting, the rate of mass loss steadily increases up to about 600 K, where the weight of the sample is reduced to roughly half. As it may have been expected, this process depends upon the scanning rate: in nitrogen, half mass is reached near 590 K at 2 K min^{-1}, near 605 K at 5 K min^{-1} and near 620 K at 10 K min^{-1}. An endothermic peak, with a maximum occurring about 70 K before half the mass is lost, has been observed in most runs.[6] The temperature of this maximum, T_{2p}, shows a logarithmic dependence on β. While T_{2p} can be determined in most runs, and does not appear to depend upon the open/pierced pan condition, the enthalpy is difficult to estimate at low heating rates, since this phenomenon may begin in the "melting region". Furthermore, in an open pan, the DSC baseline has a non-regular behavior after T_{2p} and this makes estimation of enthalpy uncertain, or impossible. For this reason, we will analyze only the enthalpy ΔH_2 of this endothermic peak, as measured in pierced containers with the Du Pont DSC. Under these conditions, this peak seems to be the last thermal event, in the sense that a flat baseline is observed afterward. A typical DSC recording is given in the inset of Fig. 6. In Fig. 6 we plot the enthalpies of the second peak, ΔH_2 (J g^{-1}) versus the enthalpy ΔH_1 of the "melting peak", as measured at scanning rates from 0.5 to 10 K min^{-1}. Quite surprisingly, variations of the two enthalpies appear to be related (correlation of 0.96), and may be described by

$$\Delta H_2 = -155 \pm 39 + (5.2 \pm 0.8)\Delta H_1 \quad (2)$$

We will discuss the meaning of this relationship in the next section.

[6] In few cases (heating rate ≤ 0.5 K min^{-1}, open pans) there was not a clear endothermic peak after the melting region.

The gaseous products of the decomposition and reaction processes have been analyzed with carefully planned TG/FT-IR experiments. The conditions of these experiments are similar to those of STA experiments (open pan under a flow of dry nitrogen). We compare the curve of weight loss and the total absorbance at 10 K min^{-1} (Fig. 7a) and 2 K min^{-1} (Fig. 7b). The curves of weight loss are similar, but the one at high β is displaced towards higher temperatures by about 30 K. The absorbance curves, instead, are very different in both shape and maximum intensity (notice the difference in vertical scales). At 10 K min^{-1}, the absorbance becomes detectable above 443 K and increases steeply from 550 K (i.e. the T_{2p} value at this rate) up to ~630 K, where more than 90% of the sample has been consumed. At 2 K min^{-1}, the absorbance increases at a roughly constant rate beginning at ~400 K and ending at ~600 K, where few percents of

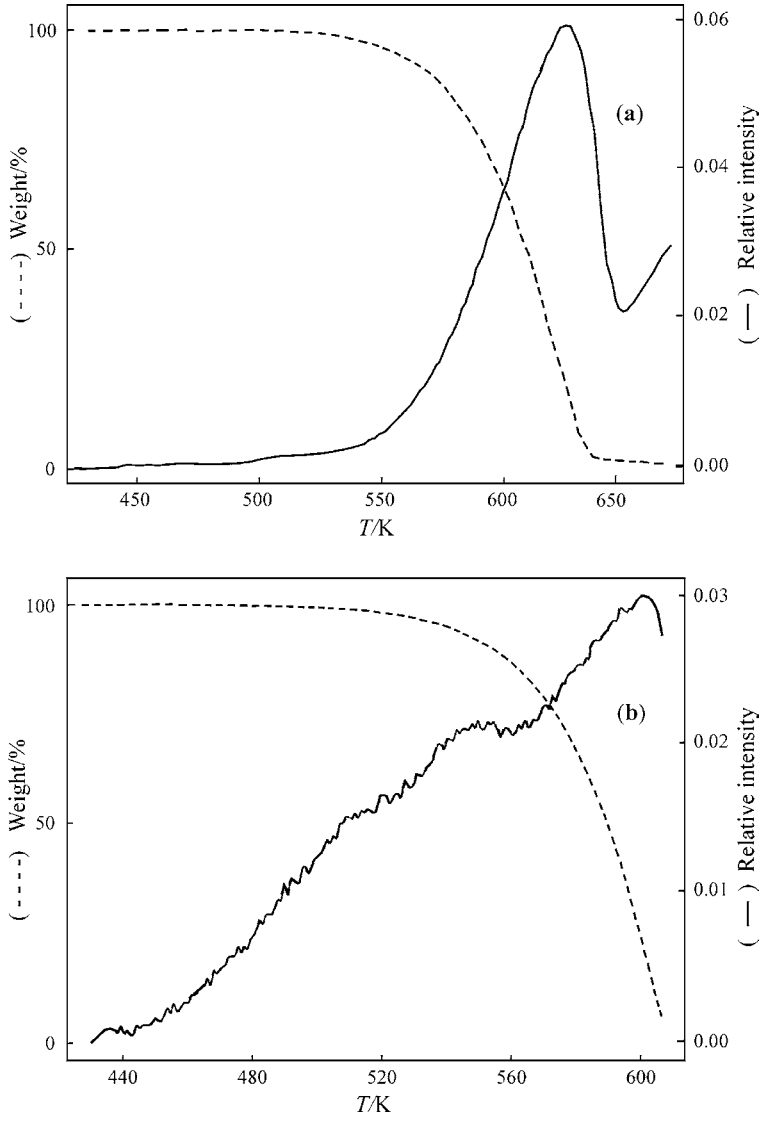

Fig. 7. Evolution of the mass (left scale) and of the relative intensity of absorption (right scale) vs. temperature in TG/FT-IR experiments performed at 10 K min^{-1} (upper part) and 2 K min^{-1} (lower part).

Table 1
TG/FT-IR experiments at two different heating rates

$\beta = 10$ K min^{-1}		$\beta = 2$ K min^{-1}	
T (K)	Products[a]	T (K)	Products[a]
453	H_2O, CO_2	447	CO_2, H_2O
		471	CO_2, H_2O
502	C=O, CO_2		
548	C=O, CO_2, H_2O, C–H		
566	C=O, CO_2, H_2O, C–H	573	H_2O, C–H, CO_2
629	C=O, CO_2, C–H, H_2O,	603	H_2O, CO_2, C–H
652	CO_2, C=O, C–H, H_2O		

[a] In order of decreasing intensity.

the sample remain in the TG cell. The absorbance curve displays "bumps" from 500 K (T_{2p} at 2 K min^{-1}) to 570 K. The differences in decomposition products observed at the two speeds are substantial, as Table 1 indicates. At low heating rates, CO_2 and H_2O are the main constituents of the evolved gases; at a high heating rate, these products are dominant only around 450 K. After melting, they are present along with carbonyl and alkane residues, i.e. not fully oxidized/decomposed fragments of spironolactone. These findings are surprising, considering that the samples are in an open container under a flow of dry nitrogen. It is hard to escape the conclusion that the oxidizing agent is produced by the decomposition process itself, a fact already suggested by a comparison of DSC results under different atmosphere.

4. Discussion

4.1. The basic model

We have shown in several ways that "decomposition" and "oxidation" occur in the melting region, and cannot be ignored when interpreting the thermal response of spironolactone. The experimental evidence suggests phenomenological expressions for the apparent enthalpy of melting, ΔH_1, and for the enthalpy ΔH_2 of the endothermic peak recorded after melting

$$\Delta H_1 \cong \Delta H_{fus} + \Delta H_d\, m_{1d} + \Delta H_o\, m_{1o} \quad (3a)$$

$$\Delta H_2 \cong \Delta H_d\, m_{2d} + \Delta H_o\, m_{2o} \quad (3b)$$

Here, ΔH_{fus} is the true enthalpy of melting while m_{1d}, m_{2d} and m_{1o}, m_{2o} are the fractions mass lost for decomposition/initial mass and mass lost for oxidation/initial mass. While we do not know these quantities, by definition, they are related to the experimentally determined fractional losses m_1 and m_2 by

$$m_{1d} + m_{1o} = m_1 \quad (4a)$$

$$m_{2d} + m_{2o} = m_2 \quad (4b)$$

Eq. (3a) implies that the entire sample undergoes melting, or that the loss of weight before/during melting is a small fraction of the initial mass, as it is the case. While decomposition and oxidation are probably complicated multi-stage processes in spironolactone, we attempt to describe them with just two constants, ΔH_d and ΔH_o, which have the following meaning

1. ΔH_d characterizes an endothermic process leading to gas formation and taking place at the same rate in any atmosphere; it is the enthalpy per gram of gas evolved due to a process that may also produce non-gaseous byproducts. In other words, ΔH_d has not the usual meaning of decomposition enthalpy.
2. ΔH_o is the enthalpy per gram of sample evolved as a gas during an exothermic reaction involving byproducts of decomposition and/or a component of the atmosphere.

Since oxidation appears to be determined by decomposition, we will express m_{1o} (m_{2o}) as a function of m_{1d} (m_{2d}) in the following way

$$m_{1o} = \alpha m_{1d}(1 - \sigma) \quad (5a)$$

$$m_{2o} = \alpha m_{2d}(1 - \sigma) \quad (5b)$$

These equations translate the following ideas.

- Oxidation cannot occur if there is no decomposition ($m_{1d} = 0$ or $m_{2d} = 0$) since it acts upon byproducts of decomposition.
- When a thermal phenomenon "ends", a portion σ of these byproducts has not been involved yet in oxidation; this parameter is expected to depend upon the atmosphere and the heating rate.
- The parameter α is the maximum attainable ratio between gaseous products of oxidation and decomposition; it may depend upon the chemistry and/or

thermodynamics of these processes, as will be discussed below.

We begin by applying the model to the "melting" phenomenon. With an open pan in nitrogen flow, the concentration of gaseous oxidants is expected to be negligible in the solid phase; m_{1o} should be nearly zero and $\sigma \cong 1$. The enthalpy versus mass data should then be fitted by the equation

$$\Delta H_1 \cong \Delta H_{fus} + \Delta H_d\, m_{1d} \approx \Delta H_{fus} + \Delta H_d\, m_1 \qquad (6)$$

A comparison with Eq. (1) confirms the interpretation of melting enthalpy for the intercept ΔH_1, the value extrapolated to a zero mass loss ($\sim$29 J g^{-1}), and of decomposition enthalpy for the slope of ΔH_d (10 kJ g^{-1}).

We may now comment the minor deviation from linearity in the ΔH_1 versus m_1 plot (see Footnote 4) at low m_1 values, corresponding to $\beta \geq 10$ K min^{-1}. We believe that the enthalpy stays the same ($\sim$50 J g^{-1}) while the lost mass varies from 0.15 to 0.35% because, with decreasing β, oxidation begins contributing to the loss of mass, thus offsetting the enthalpy increase due to the increased decomposition. This point will be further discussed in the following.

4.2. Refining the simple model

We have seen that the true melting enthalpy is $\sim$30 J g^{-1} and that, depending on experimental conditions (open-pierced pans, atmosphere, heating rate), we can measure quite different values as a consequence of the enthalpic contribution of decomposition/oxidation. Oxidation follows decomposition, but their relative enthalpic weights in the wake of melting can be greatly affected by experimental conditions, as shown by the opposite trends of ΔH_1 with decreasing heating rate in open and pierced pans. However, both in open and pierced pans, the heat flow reaches a baseline value after melting, suggesting that the thermal phenomena are over. The STA experiments clearly show that when this happens, the rate of mass loss is still increasing with temperature, meaning that decomposition/oxidation processes are far from being completed. Thus, the existence of a compensation between the endothermic and exothermic effects of decomposition and oxidation comes out as a direct experimental evidence.

If we assume that decomposition is not affected by the presence of oxygen in the measuring chamber, we may have a rough estimate of ΔH_o from Eqs. (3a) and (3b) by comparing enthalpies and mass losses in air and nitrogen at 0.5 K min^{-1} (see above). We obtain $m_o \approx 0.5\%$ and $\Delta H_o \approx -28$ kJ g^{-1}.

The experiments with the pierced pan in an inert atmosphere may qualitatively be explained as follows: at high β, the value of ΔH_1 is determined by the enthalpy of melting and by the heat of decomposition of a small (and constant) amount of sample. With decreasing β, the concentration of the decomposition byproducts increases, but, to the difference of the experiments in open pan, the concentration of oxidant is no longer negligible, and oxidation occurs also in the solid phase. However, the mechanism of compensation is still at work, and now it maintains ΔH_1 constant from about 50 to 2 K min^{-1}. However, by further lowering β, m_{1o} increases faster than m_{1d}, and this causes the observed decrease of ΔH_1 with decreasing β. We believe that, for vanishingly small scanning rates, ΔH_1 in the pierced pan will attain the ΔH_{fus} value, the reason being that oxidation appears to follow decomposition and to occur, at most, at the rate which insures an "adiabatic balance" between decomposition and oxidation. The evidence for this is that we have never observed the well-defined exothermic phenomenon expected when this oxidation rate is exceeded. If this is the case, the following interpretation of Eqs. (5a) and (5b) may be put forward. Since the maximum amount of oxidation is achieved when $\sigma = 0$, α in Eqs. (5a) and (5b) should be equal to $\Delta H_d/\Delta H_o \approx 0.36$. The dimensionless parameter σ is determined by how much, in the average, oxidation is lagging behind decomposition over the interval of integration of the heat flow. It is estimated to be of the order of 50% in the pan in air at 0.5 K min^{-1}.

4.3. The relationship between ΔH_1 and ΔH_2

The adiabatic equilibrium is dynamic in nature, and breaks down when the second endothermic phenomenon begins, presumably because of a sharp increase in the rate of decomposition. However, the compensation mechanism is always active, and the adiabatic equilibrium is rapidly restored. We have no elements to infer that this equilibrium changes with temperature, and that the α-parameters in Eqs. (5a) and (5b)

are different. Since σ is essentially due to the ''delay'' with which oxidation follows decomposition, the simplest way of modeling it is by assuming that it is a function of the scan rate (or experimental time), and not of temperature, or physical state. If this is the case, the parameter σ appearing in Eq. (5a) should be identified with that of Eq. (5b) and, for every heating rate and atmosphere we should have

$$\frac{m_{1o}}{m_{1d}} = \frac{m_{2o}}{m_{2d}} = \alpha(1-\sigma) \tag{7}$$

From Eqs. (3) and (7) it follows

$$\Delta H_2 = m_{2d}\,\Delta H_d + m_{2o}\,\Delta H_o = \bar{K}(m_{1d}\,\Delta H_d + m_{1o}\,\Delta H_o) = K(\Delta H_1 - \Delta H_{fus}) \tag{8}$$

with

$$K = \frac{m_{2d}}{m_{1d}} = \frac{m_{2o}}{m_{1o}}$$

Eq. (8) states that ΔH_2 is K times the net enthalpic contribution of decomposition/oxidation to the ''melting'' peak. A comparison of this equation with Eq. (2), which describes an experimental result, suggests that, in the ΔH_2 versus ΔH_1 plot

1. the slope should be $K = (m_{2d}/m_{1d}) = (m_{2o}/m_{1o})$;
2. the ratio between the intercept and the slope should be $-\Delta H_{fus}$ (J g^{-1}).

As the experimental values of the intercept and slope are -155 and 5.2 J g^{-1}, respectively, we obtain $\Delta H_{fus} = (155/5.2) = 29.8$, J g^{-1} i.e. the value of the true melting enthalpy we already obtained from Eq. (1) and from the experiments on annealed samples. This shows that the predictions of our model about the linkage between ΔH_2 and ΔH_1 are correct and that the physical reason of the linkage is the constant ratio of the mass losses due to decomposition and oxidation.

We now call attention to the fact that the temperatures T_{2p} and T_{1p} display a logarithmic dependence upon β over a wide range of scanning rates. We may assume that these maxima occurs when the rate of a certain reaction, or transformation, is maximum, and that amount q that transforms or reacts follows a law-of-mass

$$\frac{dq}{dt} = -\frac{q}{\tau(T)}$$

where the time constant τ has a temperature-activated behavior

$$\tau(T) \propto \exp\left(-\frac{E}{RT}\right)$$

If this is the case, an Arrhenius plot of β versus $1/T_{1,2p}$ would approximately give the activation energies of processes 1 and 2. With the T_{1p} data, we would obtain $E_1 \approx 850$ kJ mol^{-1} and $E_2 \approx 100$ kJ mol^{-1} from the T_{2p} data. These quantities are roughly of the correct order of magnitude, and probably related to the molar enthalpies of decomposition and oxidation. However, we believe that the Arrhenius plots yield apparent activation energies, which are not simply related with the characteristic bond energies of spironolactone and its byproducts.

5. Conclusions

We have given ample evidence that melting in spironolactone is always accompanied by loss of mass and thermal phenomena that can be explained in terms of ''decomposition'' and ''oxidation''. We have also shown that a good understanding of the main characteristics of these processes does not require a detailed knowledge of their chemistry and can be obtained through a simple analysis of the thermal behavior of the compound. Decomposition is endothermic, and occurs in a temperature-activated way. Oxidation follows and, perhaps, competes with decomposition; it is an exothermic reaction in which one of the reagents is a gas and the other one is produced by decomposition. The thermal behavior of spironolactone is mostly determined by the loss of mass and by the balance between decomposition and oxidation. We have shown that we have ways to control this balance, through the atmosphere and the temperature scan rate. However, even in an open pan in nitrogen, oxidation cannot be entirely avoided.

We have identified a powerful mechanism of compensation, that may be called the adiabatic equilibrium, which is the tendency of the system to achieve an enthalpic balance between decomposition and oxidation. This is actually an experimental observation, even though it may be argued that all surplus of enthalpy produced by oxidation will be naturally absorbed by the system, with no increase in

temperature, as long as the pool of substance to be decomposed has not been depleted.

We have introduced a very simple model, which appears to qualitatively capture most of the experimentally observed features, in particular, the dependence upon the heating rate and the atmosphere. We acknowledge that there is no reason to expect that the complicated and kinetically controlled decomposition/oxidation reactions are well described by their average enthalpies. However, it seems that our model works quite well.

We keep our last remark for the melting process itself, which was our original target. We have evaluated the enthalpy of melting from different experiments, and consistently found a value of about 30 J g^{-1}, substantially lower than that reported in the literature. However, we have shown that the apparent enthalpy of melting does not describe a well-defined property of the system, and only in very special circumstances it approaches the true melting enthalpy. All this has profound implications for the nature of the melting, which is a fundamentally irreversible process both from the physical point of view (formation of a glassy phase upon cooling) and the chemical point of view (unavoidable presence of decomposition).

References

[1] V. Agafonov, B. Legendre, N. Rodier, D. Wouessidjewe, J.M. Cense, J. Pharm. Sci. 80 (2) (1991) 181.
[2] S.S. El-Dalsh, A.A. El-Sayed, A.A. Badawi, F.I. Khattab, A. Fouli, Drug Dev. Ind. Pharm. 9 (5) (1983) 877.
[3] E.G. Salole, F.A. Al-Sarraj, Drug. Dev. Ind. Pharm. 11 (4) (1985) 855.
[4] V. Berbenni, A. Marini, G. Bruni, A. Maggioni, R. Riccardi, A. Orlandi, Thermochim. Acta. 340/341 (1999) 117.
[5] M. Reading, D. Elliot, V.L. Hill, J. Thermal Anal. 40 (1993) 931.
[6] P.S. Gill, S.R. Sauerbrunn, M. Reading, J. Thermal Anal. 40 (1993) 949.
[7] B. Wunderlich, Y. Lin, A. Boller, Thermochim. Acta 238 (1994) 277.
[8] A. Marini, V. Berbenni, G. Bruni, A. Maggioni, M. Villa, J. Thermal Anal. 56 (1999) 699.
[9] M. Reading, Trends Polym. Sci. 8 (1) (1993) 248.
[10] J. Cao, Thermochim. Acta 325 (1999) 101.